Available online at www.sciencedirect.com
ScienceDirect
International Journal of Pharmaceutics 339 (2007) 237–245
INTERNATIONAL JOURNAL OF PHARMACEUTICS
www.elsevier.com/locate/ijpharm

Pharmaceutical Nanotechnology

Development of carbonyl iron/ethylcellulose core/shell nanoparticles for biomedical applications

J.L. Arias [a,*], M. López-Viota [a], M.A. Ruiz [a], J. López-Viota [b], A.V. Delgado [b]

[a] *Department of Pharmacy and Pharmaceutical Technology, Faculty of Pharmacy, University of Granada, 18071 Granada, Spain*
[b] *Department of Applied Physics, Faculty of Sciences, University of Granada, Spain*

Received 8 November 2006; received in revised form 23 February 2007; accepted 26 February 2007
Available online 1 March 2007

Abstract

A reproducible method for the preparation of mixed colloidal nanoparticles, consisting of a magnetic carbonyl iron nucleus and a biocompatible ethylcellulose latex shell, is described in this article. The heterogeneous structure of the particles can confer them both the possibility of being used as drug delivery systems and the responsiveness to external magnetic fields, allowing a selective guidance of drug molecules to specific target tissues without a concurrent increase in its level in healthy tissues. The preparation method is based on an emulsion solvent evaporation process. A complete physicochemical characterization of the composite particles was carried out, and this preliminary investigation showed that the surface behavior of the core/shell particles is similar to that of bare ethylcellulose particles. This was confirmed, in particular, by zeta potential determinations as a function of pH and ionic strength. This fact points to the ethylcellulose shell efficiently coating carbonyl iron, and leading to composite particles which, from the electrokinetic point of view, are almost indistinguishable from latex. The thermodynamic analysis agrees with the electrokinetic one in suggesting that the coverage has been complete, since the components of the surface free energy of mixed particles coincide almost exactly with those corresponding to the cellulose-based pseudolatex. Moreover, the hydrophilic nature of carbonyl iron is modified and the particles become hydrophobic, just like the latex, when they are covered by ethylcellulose. The magnetic behaviors of the carbonyl iron and composite particles were also checked, and the similarities between both types of particles were demonstrated, except that the polymeric shell reduces the magnetization of the sample.

Keywords: Carbonyl iron; Drug delivery systems; Ethylcellulose; Magnetic carrier technology; Magnetic core/shell colloidal particles

1. Introduction

Because of their peculiar physical properties (biocompatibility, controllable shape and sizes, responsiveness to external magnetic fields, etc.), an increasing number of formulations of magnetic composite particles have been developed for special medical techniques, particularly, drug delivery and targeting. We are dealing with systems usually having one of the following structures: either a magnetic core coated with a biocompatible polymer, or magnetic nuclei embedded on the polymeric surface or precipitated inside the polymeric pores (Pankhurst et al., 2003; Ren et al., 2005). The magnetic core is typically made of magnetite, maghemite or carbonyl iron; and the polymeric shell has a widely diverse nature, including poly(alkylcyanoacrylate), poly(lactide), poly(lactide-co-glycolide) and poly(ε-caprolactone) (Arias et al., 2001; Pankhurst et al., 2003; Flesch et al., 2004; Flesch et al., 2005; Okassa et al., 2005; Ren et al., 2005; Arias et al., 2006).

Their use as drug carrier systems ensures a preferential location of the major drug fraction in the target tissue (limiting systemic distribution and avoiding normal tissue clearance), and drug action at the cellular or subcellular level, without adverse effects to normal cells (Häfeli, 2004; Arias et al., 2005; Gupta and Gupta, 2005).

For drug delivery applications, magnetic carriers must be water-based, biocompatible, non-toxic and non-immunogenic; in addition, the external applied field must be strong enough and focussed to retain the particles in the vasculature flow field (Tartaj et al., 2003; Häfeli, 2004). Nevertheless, one of the most important features in the design of core/shell particles is their final size. This property not only affects other physical characteristics, such as their magnetic moment (and hence their

* Corresponding author. Tel.: +34 958 24 39 00; fax: +34 958 24 89 58.
E-mail address: jlarias@ugr.es (J.L. Arias).

0378-5173/$ – see front matter © 2007 Elsevier B.V. All rights reserved.
doi:10.1016/j.ijpharm.2007.02.028

response to applied magnetic fields), but also the biological fate of the particles once they are injected to the patient. Very small (<10 nm) carriers will be rapidly removed after their extensive extravasation and renal clearance, whereas particles with diameters >200 nm will be mechanically filtrated by the spleen and removed by the cells of the reticuloendothelial system. Moreover, carrier fractions over 5 μm will induce capillary blockade (Gupta and Gupta, 2005). However, if the particles are retained by the external magnetic field in the target tissue capillaries, drug diffusion from the capillary wall into the organ (step limited by the molecular weight of the drug) will induce the therapeutic action (Maeda et al., 2003). If, in addition, this action requires extravasation, sizes between 0.5 and 5 μm may already be suitable for that process, as has been observed even after magnetic field removal (Goodwin et al., 1999; Gupta and Gupta, 2005).

The magnetic drug delivery system described in this work is composed of a magnetic nucleus (carbonyl iron) and a biocompatible polymeric shell (ethylcellulose), in order to take advantage of the properties of its two components. Carbonyl iron (Fe^0) was chosen because of its high initial susceptibility and saturation. In addition, its toxicity is quite low (LD_{50}: 50 g/kg) (Huebers et al., 1986; Devathali et al., 1991; Chua-anusorn et al., 1999; Whittaker et al., 2002). Concerning the biodegradability of the iron nuclei used in this work (average diameter of 570 ± 160 nm, see below), most particles will be eliminated mainly by renal filtration (Okon et al., 1994).

Ethylcellulose was chosen as the biocompatible polymeric shell on the magnetic particles, responsible for the drug transport and release. This is a hydrophobic polymer, widely used in pharmaceutical technology, chemically stable under storage and characterized by its lack of toxicity for patients. Ethylcellulose can be used either as a modified drug release dosage form for oral administration or as a chemoembolization agent after sterilization, due to the prevention of the rapid revascularization of the embolized area (Dubernet et al., 1990; Zinutti et al., 1996; Grattard et al., 2002; DeMerlis et al., 2005). In cancer treatment, as a result of its great tolerability and low toxicity, this cellulose-based latex has been applied to diverse tumor lesions proving an enhanced and sustained effect, prolonging the patients survival (Kato et al., 1996; Zinutti et al., 1996). A wide variety of active agents have been proposed to be delivered by this carrier, particularly 5-fluorouracil, propranolol, loratadine, ketoprofen or morphine, among others (Zinutti et al., 1996; Yamada et al., 2001; Wu et al., 2003; Morales et al., 2004; Ubrich et al., 2004; Martinac et al., 2005).

Taking into account that the inclusion of magnetic particles in polymeric substrates does not affect the toxicity of the latter and that clinical phase I trials have clearly shown the low toxicity of these selective drug delivery systems (Ibrahim et al., 1983; Lübbe et al., 1996a,b), it is interesting to investigate the applications of carbonyl iron/ethylcellulose composites in pharmaceutical technology. In this article, a reproducible technique for the preparation of core/shell particles, consisting of an iron nucleus and a latex shell, is described. The coating efficiency will be analyzed by means of electron microscopy (TEM, HRTEM, SEM), infrared absorption spectra, and electrical, thermodynamic and chemical surface properties of the mixed particles, as compared to those of the pure magnetic core and latex colloids.

2. Materials and methods

2.1. Materials

All chemicals used were of analytical quality from Panreac, Spain, except for ethylcellulose polymer (9004-57-3; supplied by ICN Biomedical Inc., USA), carbonyl iron (BASF, Germany), formamide (Aldrich, USA), and KOH and acetone (Merck, Germany). Water used in the experiments was of deionized and filtered with a Milli-Q Academic System (Millipore, France).

2.2. Methods

2.2.1. Preparation of carbonyl iron, ethylcellulose and carbonyl iron/ethylcellulose (core/shell) nanoparticles

The selection method used to obtain carbonyl iron nanoparticles with a diameter below 1 μm and narrow size distribution consisted of a gravitational separation (Arias et al., 2006). This method involves the sonication of 0.3% (w/v) Fe^0 aqueous suspensions during 5 min. After settling under gravity during 60 min, the upper 10 mm of supernatant were taken. For these separations, 1 L flasks with an internal diameter of about 90 mm were used. The conductivity of the supernatant was ∼1 μS/cm, and no other solids but carbonyl iron were in suspension. The particles were then dried at 60 °C in a vacuum oven and stored until their use.

The method followed for the preparation of colloidal ethylcellulose latex is the procedure developed by Vanderhoff et al. (1979), with slight modifications. Briefly, 4.68 g of ethylcellulose were dissolved in a mixture of organic solvents (22.57 g benzene and 4 g ethanol; this mixture has been demonstrated to be a good solvent for ethylcellulose). After 24 h at room temperature, 0.31 g of *n*-decane was added to the polymeric phase, and it acted as a stabilizer of the emulsion prepared by adding this organic solution to 94 g of a 10^{-3}N HNO_3 aqueous solution, containing 0.125% (w/v) sodium dodecyl sulphate and 0.375% (w/v) polyethylene glycol 4000. Before mixing, both phases were heated at 67.0 ± 0.5 °C, and the incorporation of the aqueous phase to the polymeric one was carried out under mechanical stirring at 8000 rpm, during 5 min. Finally, the organic solvent was evaporated at room temperature and under mechanical stirring at 2000 rpm, during 24 h, in order to eliminate the toxicity of the systems and to increase their solid content. A whitish suspension was obtained, which was then subjected to a cleaning procedure that included repeated cycles of centrifugation (20,000 rpm, Centrikon T-124 high-speed centrifuge, Kontron, France) and redispersion in Milli-Q water. In order to ensure that the suspension was sufficiently clean, the conductivity of the supernatant was measured.

Finally, the procedure followed to obtain the core/shell nanoparticles was very similar to the one described for the latex spheres, except that the aqueous phase was a 0.266% (w/v) carbonyl iron suspension in 10^{-3}N HNO_3 solution. This initial polymer/magnetic nuclei weight ratio has been shown to pro-

duce an adequate polymer shell on the magnetic nuclei (Arias et al., 2001, 2006). Cleaning was achieved by repeated magnetic separation and redispersion in Milli-Q water, until the supernatant was transparent and its conductivity indicated that the suspensions were clean of both unreacted chemicals and non-magnetic latex particles. The final solids concentration was typically around 5.6% (w/v).

The drug incorporation into the composite core/shell particles can be carried out either by dissolving it in the aqueous phase containing the magnetic particles, and then adding the organic phase as described, or by dissolving it directly in the latter. The choice of one procedure or the other will depend on the solubility properties of the drug, and its physicochemical compatibility with the polymer and the inorganic particles. In addition, a third approach would involve a surface loading on previously synthesized particles, by contacting them with a solution of the drug.

2.2.2. Characterization methods

The determination of the size and shape of the three types of synthesized particles, was achieved through analysis of TEM, dark-field HRTEM and SEM pictures, obtained using Zeiss EM 902 (Germany) transmission, STEM PHILIPS CM20 (The Netherlands) high resolution transmission and Zeiss DSM 950 (Germany) scanning electron microscopes, respectively. A preliminary inspection of the coating efficiency was carried out by these techniques. Prior to observation, dilute suspensions [approximately 0.1% (w/v)] were sonicated for 5 min, and drops of the suspension were placed on copper grids with formvar film. The grids were then dried at 35 °C in a convection oven.

The values of specific surface area of the three kinds of solids were obtained by multipoint B.E.T. nitrogen adsorption, in a Quantasorb Jr. of Quantachrome (USA). The experiments were repeated at least three times on independent samples, in all cases.

The characterization of the chemistry of the three types of particles (carbonyl iron, latex and core/shell) was carried out by means of Fourier transform infrared spectrometry data (Nicolet 20 SXB infrared spectrometer, USA) with a resolution of $2\,cm^{-1}$.

The surface electrical properties of suspensions of the three kinds of particles studied [0.1% (w/v)], were analyzed by electrophoresis measurements as a function of both pH and $NaNO_3$ concentration, using a Malvern Zetasizer 2000 (England) electrophoresis device. Measurements were performed at 25.0 ± 0.5 °C, after 24 h of contact at this temperature. The experimental uncertainty of the measurements was below 5%.

Finally, a surface thermodynamic analysis of the three kinds of particles was also carried out, using the model developed by van Oss et al., according to which the total surface free energy of any material *i* is the sum of two contributions (van Oss, 1994; Durán et al., 1996):

$$\gamma_i^{TOT} = \gamma_i^{LW} + \gamma_i^{AB} = \gamma_i^{LW} + 2\sqrt{\gamma_i^+ \gamma_i^-} \quad (1)$$

one of which, γ_i^{LW}, is the non-polar Lifshitz-van der Waals component, and the second one, γ_i^{AB} or acid–base component, is related to the electron-donor (γ_i^-) and electron-acceptor (γ_i^+) characteristics of the material. Similarly, the interfacial solid/liquid free energy, γ_{SL}^{TOT}, and its LW and AB components (γ_{SL}^{LW}, γ_{SL}^{AB}, respectively) are related to the surface free energies of both the solid (subscripts S) and the liquid (subscripts L):

$$\gamma_{SL}^{TOT} = \gamma_{SL}^{LW} + \gamma_{SL}^{AB} = \gamma_{SL}^{LW} + 2\sqrt{\gamma_S^+ \gamma_S^-} + 2\sqrt{\gamma_S^- \gamma_S^+} - 2\sqrt{\gamma_S^+ \gamma_L^-} - 2\sqrt{\gamma_S^+ \gamma_L^-} \quad (2)$$

These quantities can be related to the contact angle θ between the liquid and the solid, using the Young's equation (Adamson, 1990):

$$(1 + \cos\theta)\gamma_L^{TOT} = 2\sqrt{\gamma_S^{LW} \gamma_L^{LW}} + 2\sqrt{\gamma_S^+ \gamma_L^-} + 2\sqrt{\gamma_S^- \gamma_L^+} \quad (3)$$

The three unknowns (γ_L^{LW}, γ_L^+ and γ_L^-) can be obtained by solving the resulting system of three equations if the contact angles of three liquids of known γ_L^{LW}, γ_L^+ and γ_L^-, are measured. In our case, we used water ($\gamma_L^{LW} = 21.8$, $\gamma_L^+ = \gamma_L^- = 25.5\,mJ/m^2$), formamide ($\gamma_L^{LW} = 39.0$, $\gamma_L^+ = 2.28$, $\gamma_L^- = 39.6\,mJ/m^2$) and α-bromonaftalene ($\gamma_L^{LW} = 43.6$, $\gamma_L^+ = \gamma_L^- = 0\,mJ/m^2$), all data having been taken from van Oss (1994). The contact angles of the three liquids were determined at 25.0 ± 0.5 °C, using a Ramé-Hart 100-00 goniometer (USA), on pellets (radius: 1.3 cm) obtained by compressing the dry powders in a Spepac hydraulic press set to 10 t during 5 min.

The magnetic properties of Fe^0 and core/shell particles (first magnetization curve and hysteresis cycle) were determined with a Manics DSM-8 vibrating magnetometer, at room temperature. The field-responsive behavior of the composite particles under the influence of an external magnetic field, was analyzed by optical microscope visualization of a 0.5% (w/v) aqueous suspension under exposure to a 0.2 T permanent magnet, using a Nikon SMZ800 (Japan) stereoscopic zoom microscope.

3. Results and discussion

3.1. Particle geometry

Fig. 1a shows TEM pictures of the carbonyl iron particles obtained using the gravitational separation method. No particles with a diameter larger than 1 μm were found. Size measurements were performed on 100 particles, and a log-normal distribution was fitted to the data: as a result, the average diameter (±standard deviation) was estimated to be: 570 ± 160 nm. As observed in Fig. 1a, the particles are almost spherical. Similar observations of the composite particles (Fig. 1b) did not allow to identify clearly enough the polymer shell around the magnetic nuclei. On the contrary, dark-field HRTEM microphotographs of the mixed particles (Fig. 1c) made it possible to show that the carbonyl iron nuclei are covered by a polymeric shell ~20 nm thick. Following the same methodology described above for the bare nuclei, we found that the average diameter (±standard deviation) of the core/shell nanoparticles was 620 ± 140 nm. In order to confirm that the whitish shell ring corresponds to ethylcellulose latex, dark-field HRTEM pictures of this cellulose-based

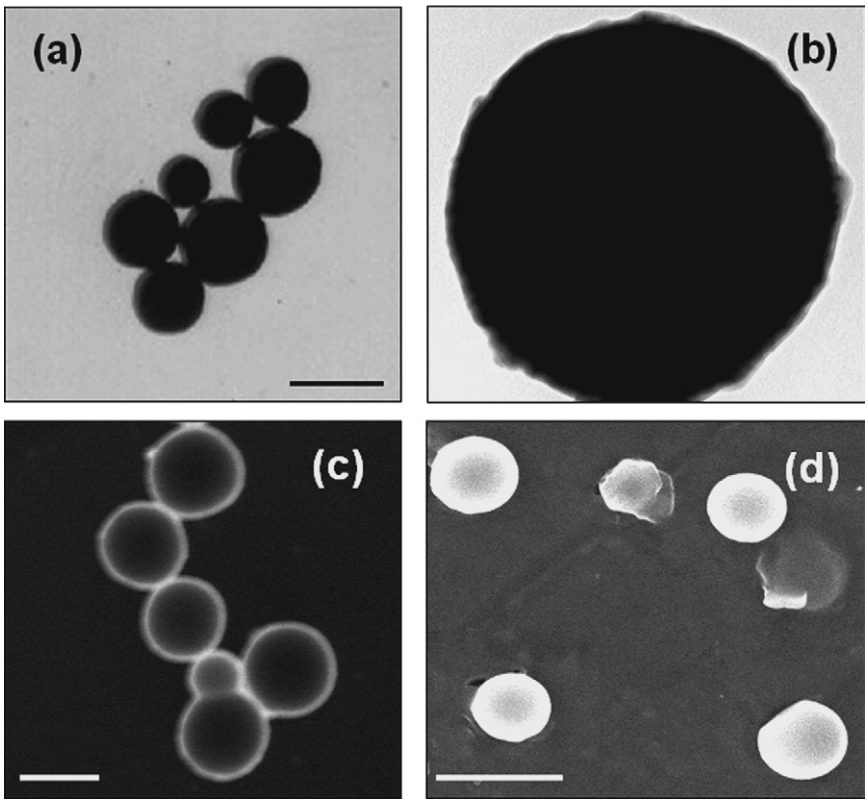

Fig. 1. Transmission electron microscope photographs of carbonyl iron (a) and core/shell particles (b), and dark-field high resolution transmission electron microscope photographs of composite particles (c) and ethylcellulose latex (d). Bar lengths: 500 nm.

polymer were also obtained. As can be seen (Fig. 1d), ethylcellulose particles appear as moderately polydisperse whitish spheres (350 ± 280 nm), thus confirming that the layer observed on the composite particles (Fig. 1c), corresponds to a latex shell.

Finally, SEM microphotographs were also obtained in order to investigate the surface texture of the three kinds of synthesized particles, with the aim of confirming the efficiency of the coverage. As can be seen in Fig. 2, the morphology and surface of the mixed nanoparticles (Fig. 2a) is identical to that of the pure polymer (Fig. 2b). This points out to a very efficient coating of the crystalline carbonyl iron by the polymeric shell.

3.2. Specific surface area

The reduction in the surface area of the iron nuclei ($1.72 \pm 0.23\ m^2/g$), when covered by the ethylcellulose latex, constitutes another proof of the coating efficiency. In fact, the specific surface areas of the ethylcellulose latex ($0.79 \pm 0.17\ m^2/g$) and core/shell ($0.86 \pm 0.08\ m^2/g$) particles is explained by the polymer layer hiding the iron nucleus, given that all the particles have similar sizes.

3.3. Chemical composition of the particles

The most significant transmittance bands of the infrared spectra of the three types of particles (Fig. 3) have been identified by comparison with data by Silverstein and Webster (1998). It can be observed that all the polymer bands are present in the mixed particles spectrum, a clear indication that the shell observed in Figs. 1b and c and 2a, corresponds indeed to an ethylcellulose coating. The small relative amount of latex in the composite sample is responsible for the reduction in the band intensity of the core/shell spectrum. The bands at 3489 and 1632 cm^{-1} correspond to the moisture content of the samples. The main groups identified are: (A) C–H stretching (2981 and 2808 cm^{-1}); (B) C–H bending (1485 and 1279 cm^{-1}); (C) C–O–C stretching (1109 and 1057 cm^{-1}); (D) medium band characteristic of alkanes (918 and 881 cm^{-1}); and finally, band E (579 cm^{-1}) indicate that the band C belongs to an ether group.

3.4. Electrokinetic characterization

The conversion of the experimental electrophoretic mobility into zeta potential values was achieved using the theory of O'Brien and White (1978). The electrokinetic study was first focussed on the pH effect on the zeta potential, ζ, for the three kinds of particles in the presence of 10^{-3} M $NaNO_3$ (Fig. 4a). Note that carbonyl iron particles show a well-defined isoelectric point (pH_{iep} or pH of zero potential) close to pH 5. The surface charge of these metal particles is originated at the metal/solution interface by the amphoteric thin oxide layer, whose formation cannot be avoided in oxidizing environments (Kallay et al., 1991; Plaza et al., 2002). Considering this value of the pH_{iep}, it can be expected that the iron particles will display a positive surface charge at the pH of the aqueous phase used in the synthesis

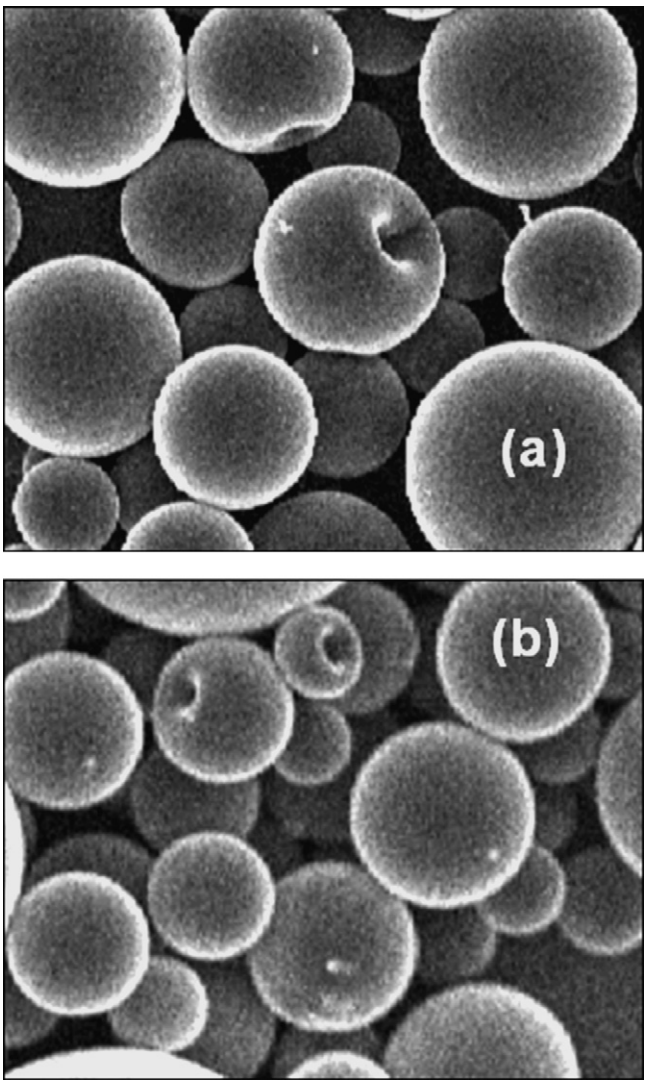

Fig. 2. Scanning electron microscope pictures of mixed particles (a) and ethylcellulose latex (b).

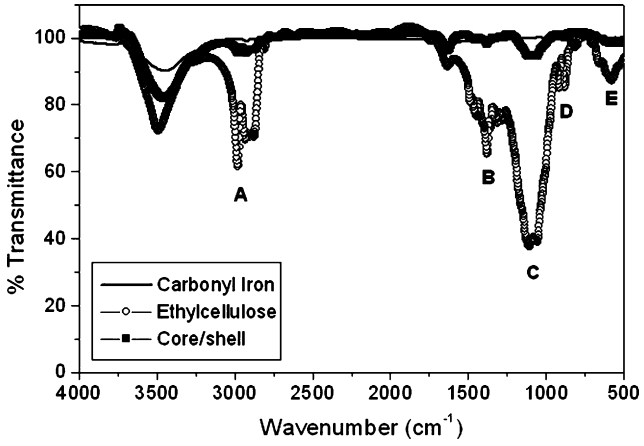

Fig. 3. Infrared spectra of carbonyl iron, ethylcellulose latex and mixed particles.

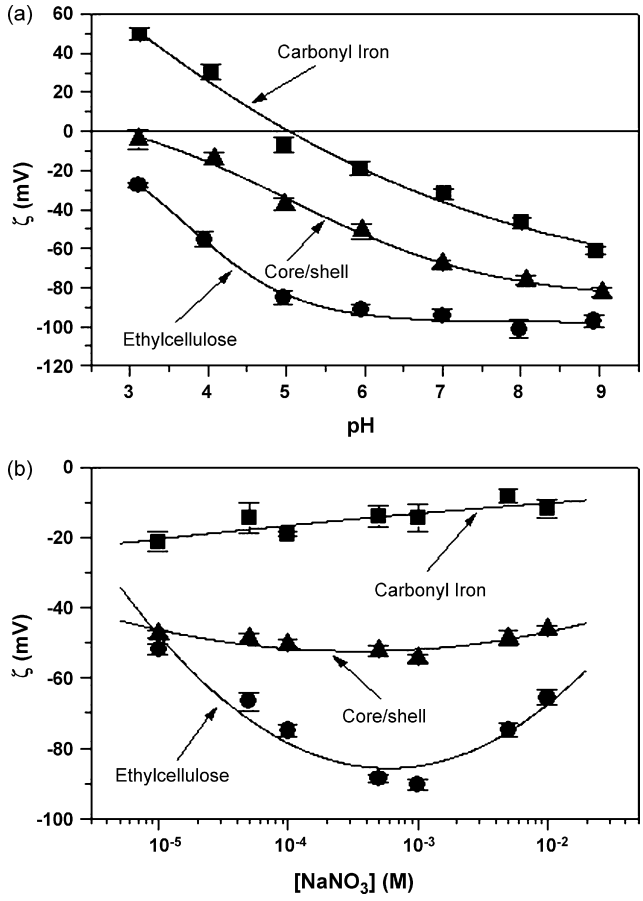

Fig. 4. Zeta potential of carbonyl iron, ethylcellulose and composite particles as a function of pH in the presence of 10^{-3} M $NaNO_3$ (a), and as a function of the $NaNO_3$ concentration at pH 5.5 (b).

of core/shell particles (pH ≈ 3) (Matijević, 2002; Flesch et al., 2005).

However, ethylcellulose particles have a negative surface charge for the whole pH range studied and only at pH < 3, the zeta potential can approach a zero value. This behavior can be explained if we take into account the charge generation mechanism at the polymer/solution interface and the results obtained with Aquacoat®, a latex similar to ethylcellulose (Gallardo et al., 1993; Vera et al., 1994, 1996). The generation of the negative surface charge is due to strong groups corresponding to dissociated end molecules of the sodium dodecyl sulfate used in the synthesis, that remain adsorbed on the particle surface even after the cleaning procedure. In addition, weak acid groups, presumably carboxylic, must be responsible for the pH-dependence of the surface charge (Gallardo et al., 2005).

This electrokinetic technique is a very useful tool for qualitatively checking the coating efficiency, due to the large differences between nuclei and polymer particle mobilities and zeta potentials. In fact, Fig. 4a clearly shows that the ζ–pH trends of mixed particles are dominated to a large extent by the latex shell. This must be a consequence of a suitable polymeric coating of Fe^0, leading to composite particles which, from an electrokinetic point of view, are qualitatively similar to ethylcellulose.

We also measured ζ as a function of $NaNO_3$ concentration at a constant pH 5.5, in order to confirm these results. This is shown in Fig. 4b for the three kinds of particles. Note that the effect of $NaNO_3$ concentration on each of the particles is different, not only considering the average mobility values, but also the ζ–concentration trends. Fig. 4b shows that iron has the lowest $|\zeta|$ values, ethylcellulose the largest ones, and, as before, the composite particles yield intermediate zeta potentials, closer to those of the polymer than of the iron nuclei. This was expected considering the zeta potentials at pH 5.5 for the three colloidal systems (Fig. 4a). Of a greater interest is the fact that $|\zeta|$ changes differently with the ionic strength: in the case of iron, a decrease in the absolute value of zeta potential is observed when $NaNO_3$ is increased, a consequence of the classical double-layer compression mechanism, in virtue of which the electric potential decreases faster with distance the larger the indifferent electrolyte concentration. However, the latex particles (and, to a lesser extent, also the composite ones) display a quite different trend: $|\zeta|$ goes through a maximum, so that only at high enough $NaNO_3$ concentration is the compression observed. Several explanations have been given to the initial increase of $|\zeta|$ with concentration, but it seems to be clear that this is a manifestation of stagnant-layer conductivity (Lyklema, 2002). This means electrical conduction (but not liquid motion) in the inner part of the double layer: ions flow tangentially to the particle, without dragging liquid, when a field is applied. As a consequence, the particle velocity is larger (the particle is less breaked if the liquid flow against its motion is weaker) and leads to an apparently larger zeta potential. This effect is obviously less important if the diffuse region is richer in counterions (this will happen if the bulk concentration of ions is large enough), and the classical behavior is recovered at high $NaNO_3$ concentrations.

Electrokinetics can also help in elucidating the mechanisms through which the ethylcellulose layer is formed on the carbonyl iron surface: it is clear that an attractive electrostatic interaction will exist between the positively charged Fe^0 particles and the negatively charged polymer, at the acidic conditions in which the synthesis is performed (see Fig. 4a). Because of this attraction, the vicinity of the carbonyl iron surface will be enriched in polymer species, negative at that pH range.

3.5. Surface thermodynamics

The analysis of the surface free energy components of the three types of particles was used to check the nature of the ethylcellulose coating. The contact angle data of the three probe liquids on particles pellets already suggest significant differences among the three types of nanoparticles (Table 1). But it is the evaluation of the γ_S components, that provides a better physical characterization of their surface thermodynamics (Table 2). As can be seen, whatever the component considered, its values for the mixed particles are similar to those for the bare latex (γ_S^+ is not suitable for the comparison, as it displays values close to zero in the three cases). In addition, γ_S^{LW} for the composite particles is almost the same as that of ethylcellulose, although this component is the least affected (as it is usually the case, see, e.g. Plaza et al., 1998; Arias et al., 2001, 2006). However, γ_S^- shows large values in carbonyl iron, that is thus essentially a monopolar, electron-donor material. Its value of γ_S^- is larger than that found for either the polymer or the core/shell. This thermodynamic analysis agrees with the electrokinetic one in suggesting that sufficient coverage has been achieved, since the γ_S components of mixed particles coincide almost exactly with those corresponding to ethylcellulose.

Table 1
Contact angle θ (degrees) of the probe liquids indicated on carbonyl iron, ethylcellulose and carbonyl iron/ethylcellulose (core/shell) particles

Solid	Liquid		
	Water	Formamide	α-Bromonaftalene
Carbonyl iron	27.9 ± 1.1	21.5 ± 0.7	16.7 ± 0.5
Ethylcellulose	65.3 ± 0.7	62.9 ± 0.8	30.1 ± 3.1
Ethylcellulose/Fe^0	64.1 ± 1.3	60.3 ± 1.5	29.4 ± 1.2

Table 2
Surface free energy components of carbonyl iron, ethylcellulose and carbonyl iron/ethylcellulose (core/shell) particles

	γ_S^{LW}	γ_S^+	γ_S^-
Carbonyl iron	41.8 ± 0.1	0.75 ± 0.01	45.4 ± 0.8
Ethylcellulose	37.9 ± 1.1	0.41 ± 0.05	26.7 ± 0.4
Ethylcellulose/Fe^0	38.2 ± 0.4	0.22 ± 0.05	26.1 ± 0.6

γ_S^{LW} is the Lifshitz-van der Waals component; γ_S^+ (γ_S^-) is the electron-acceptor (electron-donor) component. All values are in mJ/m^2.

These surface free energy changes manifest themselves in the hydrophobicity/hydrophilicity characteristics of the different materials. The evaluation of the free energy of interaction ΔG_{SLS} (not considering the electrostatic component) between the solid phases immersed in the liquid, can be used to check whether a material can be considered hydrophobic or hydrophilic (van Oss, 1994). This can be written, per unit area of interacting particles, as follows:

$$\Delta G_{SLS} = -2\gamma_{SL}^{TOT} \quad (4)$$

If this quantity is found to be negative, interfacial interactions will favor attraction of the particles to each other, and they are hence considered hydrophobic. On the opposite case,

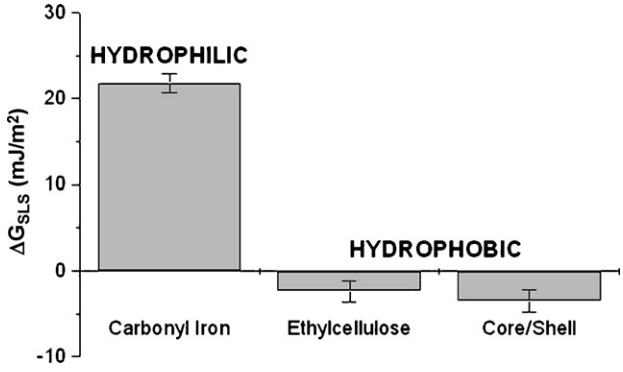

Fig. 5. ΔG_{SLS} (solid–liquid interfacial energy of interaction) values and hydrophobicity/hydrophilicity of the three types of particles.

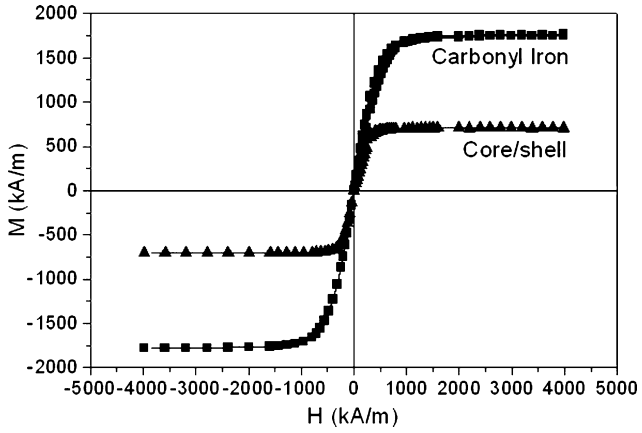

Fig. 6. Hysteresis cycles of the carbonyl iron and core/shell nanoparticles.

hydrophilicity will correspondingly be associated to positive values of ΔG_{SLS}^{TOT}. As observed in Fig. 5, the hydrophilic nature of carbonyl iron is modified and the core becomes hydrophobic (just like the latex) when covered by ethylcellulose.

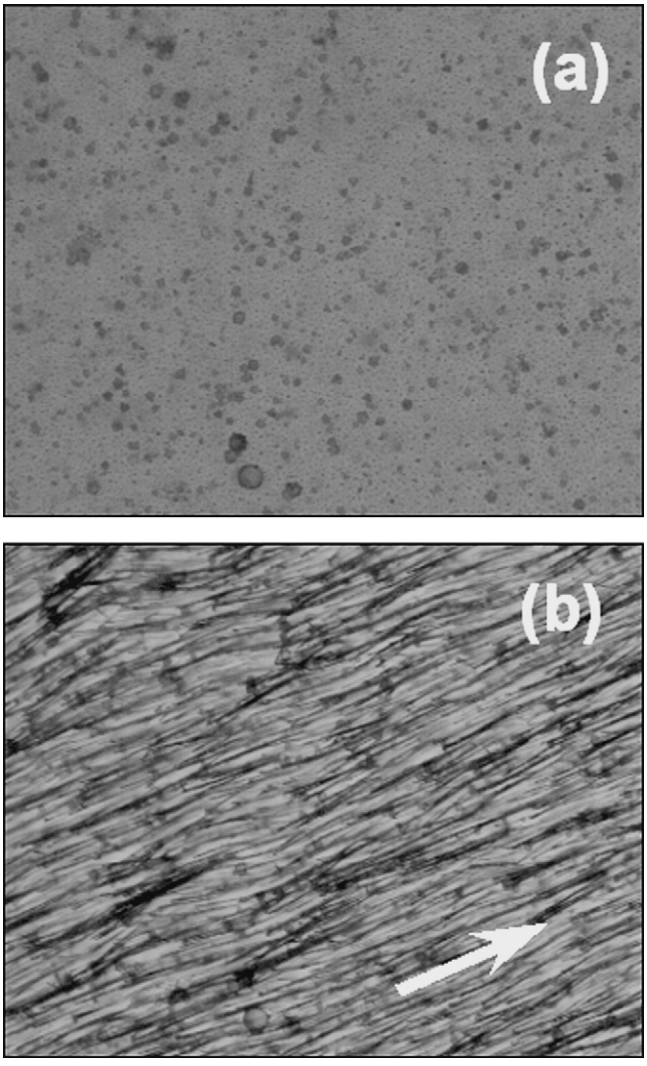

Fig. 7. Optical microscope photographs (magnification 63×) of a core/shell nanoparticle suspension without (a) and under the influence (b) of an external magnetic field, $B = 0.2$ T, in the direction of the arrow.

3.6. Magnetic properties

We considered also of interest to analyze to what extent the magnetic properties of the iron nuclei remain in the composites. The hysteresis cycles of both the carbonyl iron nuclei and the mixed particles reveal their soft magnetic behavior (Fig. 6), and in fact the increasing and decreasing branches of the hysteresis cycles are hardly distinguishable, considering the sensitivity of our magnetometer. As previously observed (Arias et al., 2005, 2006; Ren et al., 2005), the magnetic behavior of composite nanoparticles is similar to that of the nuclei, except that the polymeric shell reduces the magnetization of the sample. From the linear portions (low field) of the curves in Fig. 6, we could estimate the initial susceptibility, $\chi_i = 22.1 \pm 0.2$ for carbonyl iron and $\chi_i = 9.1 \pm 0.1$ for core/shell particles. It is also significant the reduction of saturation magnetization brought about by the ethylcellulose layer: 1698 ± 5 kA/m for carbonyl iron (close to published data obtained with 6 μm particles, see Phulé et al., 1999; Arias et al., 2006), and 703.3 ± 0.8 kA/m for composite particles.

Finally, the response of composite particles to external magnetic fields was evaluated by optical microscopy inspection of an aqueous suspension under exposure to a magnetic field. As can be seen in Fig. 7, the initially homogeneous distribution of particles is strongly modified, and formation of chainlike aggregates parallel to the field lines is observed. This is due to the fact that the magnetic interaction represents a significant contribution over the DLVO colloidal interactions between core/shell particles (electrostatic van der Waals and hydration or acid–base), in spite of the presence of the polymer shell.

4. Conclusions

In this work, a reproducible method is described for coating magnetic colloidal particles with a biocompatible ethylcellulose shell. Although the existence of this shell is observable under the electron microscope, the efficiency of the coating is demonstrated by the comparison of the thermodynamic and electrophoretic surface analysis of the mixed particles with those of their components. The electrical surface properties of carbonyl iron are almost completely controlled by the polymer coating and the surface thermodynamics analyses confirm this conclusion: the originally hydrophilic carbonyl iron changes to hydrophobic when coated by ethylcellulose. Finally, despite the observed reduction in magnetic strength, the core/shell particles constitute an ideal candidate to be used for drug delivery: their surface is comparable to that of the pure polymer, but they have the property of being magnetizable.

Acknowledgements

Financial supports from CICYT, Spain, under Project MAT2005-07746-CO2-02, from Junta de Andalucía, Spain, under Project FQM 410, and from FEDER Funds are gratefully acknowledged.

References

Adamson, A.W., 1990. Physical Chemistry of Surfaces, fifth ed. John Wiley & Sons, New York.

Arias, J.L., Gallardo, V., Gómez-Lopera, S.A., Plaza, R.C., Delgado, A.V., 2001. Synthesis and characterization of poly(ethyl-2-cyanoacrylate) nanoparticles with a magnetic core. J. Control. Rel. 77, 309–321.

Arias, J.L., Gallardo, V., Gómez-Lopera, S.A., Delgado, A.V., 2005. Loading of 5-fluorouracil to poly(ethyl-2-cyanoacrylate) nanoparticles with a magnetic core. J. Biomed. Nanotechnol. 1, 214–223.

Arias, J.L., Gallardo, V., Linares-Molinero, F., Delgado, A.V., 2006. Preparation and characterization of carbonyl iron/poly(butylcyanoacrylate) core/shell nanoparticles. J. Colloid Interface Sci. 299, 599–607.

Chua-anusorn, W., Macey, D.J., Webb, J., de la Motte Hall, P., St. Pierre, T.G., 1999. Effects of prolonged iron loading in the rat using both parenteral and dietary routes. Biometals 12, 103–113.

DeMerlis, C.C., Schoneker, D.R., Borzelleca, J.F., 2005. A subchronic toxicity study in rats and genotoxicity tests with an aqueous ethylcellulose dispersion. Food Chem. Toxicol. 43, 1355–1364.

Devathali, S.D., Gordeuk, V.R., Brittenham, G.M., Bravo, J.R., Hughes, M.A., Keating, L.J., 1991. Bioavailability of carbonyl iron: a randomized, double-bind study. Eur. J. Haematol. 46, 272–278.

Dubernet, C., Rouland, J.C., Benoit, J.P., 1990. Comparative study of two ethylcellulose forms (raw material and microspheres) carried out through thermal analysis. Int. J. Pharm. 64, 99–107.

Durán, J.D.G., Ontiveros, A., Delgado, A.V., González-Caballero, F., Chibowski, E.J., 1996. A study on the adhesion of calcium carbonate to glass: energy balance in the deposition process. Adhesion Sci. Technol. 10, 847–868.

Flesch, C., Delaite, C., Dumas, P., Bourgeat-Lami, E., Duguet, E., 2004. Grafting of poly(ε-caprolactone) onto maghemite nanoparticles. J. Polym. Sci. Part A: Polym. Chem. 42, 6011–6020.

Flesch, C., Bourgeat-Lami, E., Mornet, S., Duguet, E., Delaite, C., Dumas, P., 2005. Synthesis of colloidal superparamagnetic nanocomposites by grafting poly(ε-caprolactone) from the surface of organosilane-modified maghemite nanoparticles. J. Polym. Sci. Part A: Polym. Chem. 43, 3221–3231.

Gallardo, V., Salcedo, J., Vera, P., Delgado, A.V., 1993. Electric and adsorption properties of pharmaceutical polymers. Part I: electrokinetics of aquacoat. Colloid Polym. Sci. 271, 967–973.

Gallardo, V., Morales, M.E., Ruiz, M.A., Delgado, A.V., 2005. An experimental investigation of the stability of ethylcellulose latex: correlation between zeta potential and sedimentation. Eur. J. Pharm. Sci. 26, 170–175.

Goodwin, S., Peterson, C., Hoh, C., Bittner, C., 1999. Targeting and retention of magnetic targeted carriers (MTCs) enhancing intra-arterial chemotherapy. J. Magn. Magn. Mater. 194, 132–139.

Grattard, N., Pernin, M., Marty, B., Roudaut, G., Champion, D., Le Meste, M., 2002. Study of release kinetics of small and high molecular weight substances dispersed into spray-dried ethylcellulose microspheres. J. Control. Rel. 84, 125–135.

Gupta, A.K., Gupta, M., 2005. Synthesis and surface engineering of iron oxide nanoparticles for biomedical applications. Biomaterials 26, 3995–4021.

Häfeli, U.O., 2004. Magnetically modulated therapeutic systems. Int. J. Pharm. 277, 19–24.

Huebers, H.A., Brittenham, G.M., Csiba, E., Finch, C.A., 1986. Absorption of carbonyl iron. J. Lab. Clin. Med. 108, 473–478.

Ibrahim, A., Couvreur, P., Roland, M., Speiser, P., 1983. New magnetic drug carrier. J. Pharm. Pharmacol. 35, 59–61.

Kallay, N., Torbić, Ž., Golić, M., Matijević, E., 1991. Determination of the isoelectric points of several metals by an adhesion method. J. Phys. Chem. 95, 7028–7032.

Kato, T., Sato, K., Sasaki, R., Kakinuma, H., Moriyama, M., 1996. Targeted cancer chemotherapy with arterial microcapsule chemoembolization: review of 1013 patients. Cancer Chemother. Pharmacol. 37, 289–296.

Lübbe, A.S., Bergemann, C., Riess, H., Schriever, F., Reichardt, P., Possinger, K., Matthias, M., Doerken, B., Herrmann, F., Guertler, R., Hohenberger, P., Haas, N., Sohr, R., Sander, B., Lemke, A.J., Ohlendorf, D., Huhnt, W., Huhn, D., 1996a. Clinical experiences with magnetic drug targeting: a phase I study with 4′-epidoxorubicin in 14 patients with advanced solid tumors. Cancer Res. 56, 4686–4693.

Lübbe, A.S., Bergemann, C., Huhnt, W., Fricke, T., Riess, H., Brock, J.W., Huhn, D., 1996b. Preclinical experiences with magnetic drug targeting: tolerance and efficacy. Cancer Res. 56, 4694–4701.

Lyklema, J., 2002. The role of surface conduction in the development of electrokinetics. In: Delgado, A.V. (Ed.), Interfacial Electrokinetics and Electrophoresis. Marcel Dekker, New York, pp. 87–98.

Maeda, H., Fang, J., Inutsuka, T., Kitamoto, Y., 2003. Vascular permeability enhancement in solid tumor: various factors, mechanisms involved and its applications. Int. Immunopharmacol. 3, 319–328.

Martinac, A., Filipović-Grčić, J., Voinovich, D., Perissutti, B., Franceschinis, E., 2005. Development and bioadhesive properties of chitosan-ethylcellulose microspheres for nasal delivery. Int. J. Pharm. 291, 69–77.

Matijević, E., 2002. A critical review of the electrokinetics of monodispersed inorganic colloids. In: Delgado, A.V. (Ed.), Interfacial Electrokinetics and Electrophoresis. Marcel Dekker, New York, pp. 199–218.

Morales, M.E., Gallardo-Lara, V., Calpena, A.C., Doménech, J., Ruiz, M.A., 2004. Comparative study of morphine diffusion from sustained release polymeric suspensions. J. Control. Rel. 95, 75–81.

O'Brien, R.W., White, L.R., 1978. Electrophoretic mobility of a spherical colloidal particle. J. Chem. Soc. Faraday Trans. 2, 1607–1626.

Okassa, L.N., Marchais, H., Douziech-Eyrolles, L., Cohen-Jonathan, S., Soucé, M., Dubois, P., Chourpa, I., 2005. Development and characterization of sub-micron poly(D,L-lactide-co-glycolide) particles loaded with magnetite/maghemite nanoparticles. Int. J. Pharm. 302, 187–196.

Okon, E., Pouliquen, D., Okon, P., Kovaleva, Z.V., Stepanova, T.P., Lavit, S.G., Kudryavtsev, B.N., Jallet, P., 1994. Biodegradation of magnetite dextran nanoparticles in the rat. A histologic and biophysical study. Lab. Invest. 71, 895–903.

Pankhurst, Q.A., Connolly, J., Jones, S.K., Dobson, J., 2003. Applications of magnetic nanoparticles in biomedicine. J. Phys. D: Appl. Phys. 36, R167–R181.

Phulé, P.P., Mihalcin, M.T., Gene, S., 1999. The role of dispersed-phase remnant magnetization on the redispersability of magnetorheological fluids. J. Mater. Res. 14, 3037–3041.

Plaza, R.C., Zurita, L., Durán, J.D.G., González-Caballero, F., Delgado, A.V., 1998. Surface thermodynamics of hematite/ytrium terization of nanoparticles with different alkyl chain length, oxide core–shell colloidal particles. Langmuir 14, 6850–6854.

Plaza, R.C., Arias, J.L., Espín, M., Jiménez, M.L., Delgado, A.V., 2002. Aging effects in the electrokinetics of colloidal iron oxides. J. Colloid Interface Sci. 245, 86–90.

Ren, J., Hong, H.-Y., Ren, T.-B., Teng, X.-R., 2005. Preparation and characterization of magnetic PLA–PEG composite particles. Mater. Lett. 59, 2655–2658.

Silverstein, R.M., Webster, F.X., 1998. Spectrometric Identification of Organic Compounds, sixth ed. John Wiley & Sons, New York.

Tartaj, P., Morales, M.P., Veintemillas-Verdaguer, S., González-Carreño, T., Serna, C.J., 2003. The preparation of magnetic nanoparticles for applications in biomedicine. J. Phys. D: Appl. Phys. 36, R182–R197.

Ubrich, N., Bouillot, P., Pellerin, C., Hoffman, M., Maincent, P., 2004. Preparation and characterization of propranolol hydrochloride nanoparticles: a comparative study. J. Control. Rel. 97, 291–300.

van Oss, C.J., 1994. Interfacial Forces in Aqueous Media. Marcel Dekker Inc., New York.

Vanderhoff, J.W., El-Aasser, M.S., Ugelstad, J., 1979. Polymer emulsification process. U.S. Patent No. 4,177,177, December 4, 1979.

Vera, P., Taleb, A.B., Salcedo, J., Gallardo, V., 1994. Adsorption of hydrolysable cations at the aquacoat/water interface. An electrokinetic study. Colloids Surf. A: Physicochem. Eng. Aspects 92, 169–173.

Vera, P., Gallardo, V., Salcedo, J., Delgado, A.V., 1996. Colloidal stability of a pharmaceutical latex: experimental determinations and theoretical predictions. J. Colloid Interface Sci. 177, 553–560.

Whittaker, P., Ali, S.F., Imam, S.F., Dunkel, V.C., 2002. Acute toxicity of carbonyl iron and sodium iron EDTA compared with ferrous sulfate in young rats. Regul. Toxicol. Pharmacol. 36, 280–286.

Wu, P.-C., Huang, Y.-B., Chang, J.-I., Tsai, M.-J., Tsai, Y.-H., 2003. Preparation and evaluation of sustained release microspheres of potassium chloride prepared with ethylcellulose. Int. J. Pharm. 260, 115–121.

Yamada, T., Onishi, H., Machida, Y., 2001. Sustained release ketoprofen microparticles with ethylcellulose and carboxymethylethylcellulose. J. Control. Rel. 75, 271–282.

Zinutti, C., Kedzierewicz, F., Hoffamn, M., Benoit, J.P., Maincent, P., 1996. Influence of the casting solvent on the physico-chemical properties of 5-fluorouracil loaded microspheres. Int. J. Pharm. 133, 97–105.